

Dual inhibition of histone deacetylases and phosphoinositide 3-kinases: effects on Burkitt lymphoma cell growth and migration

Ana Carolina dos Santos Ferreira,* Julio Cesar Madureira de-Freitas-Junior,[†]
Jose Andres Morgado-Díaz,[†] Anne J. Ridley,[‡] and Claudete Esteves Klumb*¹

*Programa de Pesquisa em Hemato-Oncologia Molecular, Laboratório de Hemato-oncologia Celular e Molecular, and [†]Programa de Biologia Celular, Laboratório de Biologia Estrutural-Instituto Nacional de Câncer, Rio de Janeiro, Brazil; and [‡]Randall Division of Cell and Molecular Biophysics, King's College London, United Kingdom

RECEIVED APRIL 17, 2015; REVISED SEPTEMBER 14, 2015; ACCEPTED OCTOBER 19, 2015. DOI: 10.1189/jlb.2A0415-162R

ABSTRACT

Burkitt lymphoma is a highly aggressive non-Hodgkin lymphoma that is characterized by MYC deregulation. Recently, the PI3K pathway has emerged as a cooperative prosurvival mechanism in Burkitt lymphoma. Despite the highly successful results of treatment that use high-dose chemotherapy regimens in pediatric Burkitt lymphoma patients, the survival rate of pediatric patients with progressive or recurrent disease is low. PI3Ks are also known to regulate cell migration, and abnormal cell migration may contribute to cancer progression and dissemination in Burkitt lymphoma. Little is known about Burkitt lymphoma cell migration, but the cooperation between MYC and PI3K in Burkitt lymphoma pathogenesis suggests that a drug combination could be used to target the different steps involved in Burkitt lymphoma cell dissemination and disease progression. The aim of this study was to investigate the effects of the histone deacetylase inhibitor suberoylanilide hydroxamic acid combined with the PI3K inhibitor LY294002 on Burkitt lymphoma cell growth and migration. The combination enhanced the cell growth inhibition and cell-cycle arrest induced by the PI3K inhibitor or histone deacetylase inhibitor individually. Moreover, histone deacetylase inhibitor/PI3K inhibitor cotreatment suppressed Burkitt lymphoma cell migration and decreased cell polarization, Akt and ERK1/2 phosphorylation, and leads to RhoB induction. In summary, the histone deacetylase inhibitor/PI3Ki combination inhibits cell proliferation and migration via alterations in PI3K signaling and histone deacetylase activity, which is involved in the acetylation

of α -tubulin and the regulation of RhoB expression. *J. Leukoc. Biol.* **99**: 569–578; 2016.

Introduction

BL is a highly aggressive B-NHL and is the most common NHL in children. BL is characterized by MYC deregulation as a result of chromosomal translocations to the Ig enhancer regions t(8;14) (q24;q32), t(2;8) (p12;q24), and t(8;22) (q24;q11). The result of these MYC translocations is aberrant cell proliferation and survival [1]. However, the overexpression of MYC alone is not sufficient to BL pathogenesis. Recently, the PI3K/Akt pathway has been reported to contribute to BL proliferation, suggesting this pathway as a drug target for BL treatment as a result of its regulation of cell survival, growth, and migration [2, 3].

Cell migration is fundamental for many biologic processes and has been studied extensively in vitro and in vivo. The Rho GTPase family plays an important role in regulating cell migration and morphology and actin cytoskeleton organization in a positive feedback loop with PI3K, which is involved in maintaining cell polarity at the leading edge during cell migration [4]. Cell migration has been reported to contribute to cancer progression, and BL patients may present with extranodal disease in sites such as BM or the CNS, which is associated with poor prognosis [5]. Although little is known about BL migration, the hypothesis that MYC and PI3K cooperate during BL pathogenesis was validated by studies targeting MYC and activating PI3K pathway in mice. This new in vivo model is particularly attractive for the study of the mechanisms that control dissemination of BL into the CNS and the testicles [2, 6, 7].

Recently, we found that an HDACi enhances the inhibitory effects of chemotherapy on BL cell growth and is involved in alterations in the PI3K/Akt axis [7]. Given the role of HDACs in cell growth and the involvement of PI3K/Akt activity in HDACi

Abbreviations: ALL = acute lymphoblastic leukemia, B-NHL = B-non-Hodgkin lymphoma, BL = Burkitt lymphoma, BM = bone marrow, CLL = chronic lymphocytic leukemia, DLBCL = diffuse large B cell lymphoma, FOXO1/3 = forkhead box O1/O3, HDAC = histone deacetylase, HDACi = histone deacetylase inhibitor, LY = LY294002, miR = microRNA, mTOR = mammalian target of rapamycin, NHL = non-Hodgkin lymphoma,

(continued on next page)

The online version of this paper, found at www.jleukbio.org, includes supplemental information.

1. Correspondence: Laboratório de Hemato-Oncologia Celular e Molecular, Programa de Pesquisa em Hemato-Oncologia Molecular, Instituto Nacional de Câncer, Praça Cruz Vermelha, 23/6th Floor, CEP: 20 230-130, Rio de Janeiro, Brazil. E-mail: cklumb@inca.gov.br

response, it is plausible that the combined blockade of PI3K/Akt signaling and HDAC activity may affect cell growth and migration. Thus, the aim of this study was to investigate the effects of SAHA, the most commonly clinically used HDACi [8], combined with the PI3Ki LY on BL cell growth and migration.

MATERIALS AND METHODS

Cell culture

The BL cell line Daudi was kindly provided by Dr. Boulanger (Greehey Children's Cancer Research Institute, The University of Texas Health Science Center, San Antonio, TX, USA), and BL Namalwa cells were kindly provided by Dr. Favaro (Laboratório de Biologia Molecular e Celular, Hemocentro, Unicamp, Campinas, São Paulo, Brazil). Both cell lines contain the EBV genome. These cell lines were mycoplasma negative and were used within 6 mo of receipt from the source. The cells were maintained in a humidified atmosphere containing 95% air and 5% CO₂ at 37°C and were cultured in RPMI-1640 medium supplemented with 25 mM HEPES buffer (Sigma-Aldrich, St. Louis, MO, USA) and 10% heat-inactivated FCS (Gibco, Thermo Fisher Scientific, Grand Island, NY, USA).

Cell viability determined by MTT and Trypan blue exclusion assays

To evaluate the effects of SAHA and LY on cell viability, Daudi and Namalwa cells were seeded at 1×10^5 cells/well in 96-well plates in culture medium supplemented with 10% FCS. The cells were treated with SAHA (0.1–5 μ M) and/or LY (1–10 μ M). After 24, 48, or 72 h, viable cells were detected by use of MTT. The formazan crystals were solubilized with DMSO and absorbance measured at 570 nm. Three replicate wells were used for each data point. In the Trypan blue assay, the cells were collected via centrifugation after 48 h of single or combined treatment (0.5 μ M SAHA, 5 μ M LY, or both). An aliquot of the cells was combined with Trypan blue dye at a concentration of 0.04% (w/v) and was microscopically analyzed on a Neubauer counting chamber. The blue cells were counted as nonviable, and the cells lacking the blue dye were counted as viable. Cell viability was expressed as a percentage of untreated cells.

Combination index calculations were analyzed following the procedure developed by Fischel et al. [9], with the equation adapted from the method developed by Chou and Talalay [10]

$$R = \frac{\text{Survival or migration (SAHA + LY)}}{\text{Survival or migration (SAHA alone)} \times \text{survival or migration (LY alone)}}$$

According to Fischel et al. [9], if 1) $R < 0.8$, then the association is considered to be synergistic; 2) $0.8 < R < 1.2$, then the association is considered to be additive; 3) $R > 1.2$, then the association is considered to be antagonistic, where R is a replacement of the Chou Talalay confidence interval when the dose–effect curve does not reach the zero value for survival.

Cell cycle analysis

After treating Daudi and Namalwa cells with 0.5 μ M SAHA, alone or in combination with 5 μ M LY for 48 h, the cells were harvested, washed in PBS, and incubated in 500 μ l PI staining solution (50 μ g/ml PI diluted in 4 mM citrate buffer and 0.3% Triton X-100) and RNase (100 μ g/ml ribonuclease A diluted in 40 mM citrate buffer) for 15 min at room temperature. The DNA content was determined by collecting 10,000 events for cell cycle analysis by use of a CyAn ADP flow cytometry analyzer and Summit v4.3 software (Dako, Carpinteria, CA, USA).

(continued from previous page)

NSCLC = nonsmall cell lung cancer, PI = propidium iodide, PI3Ki = PI3K inhibitor, PTEN = phosphatase and tensin homolog, qRT-PCR = quantitative RT-PCR, SAHA = suberoylanilide hydroxamic acid

Migration assay

The cell migration assays were performed in triplicate by use of 8 μ m pore transwells (Costar, Corning, NY, USA), as described previously [11]. The transwells were washed twice with PBS and blocked with 0.5% BSA in RPMI 1640 for 1 h at 37°C. The lower compartment was filled with 600 μ l migration medium (0.5% BSA in RPMI medium) containing 100 ng/ml CXCL12. The cells (5×10^5 in 100 μ l migration medium) were applied to the upper compartment and allowed to migrate for 24 or 48 h. Where indicated, 0.5 μ M SAHA, 5 or 10 μ M LY, or the combination of SAHA/LY was added. The number of migrated cells was counted and expressed as a percentage of the input, i.e., the number of cells applied directly to the upper compartment in parallel wells. The percentage of migrated cells was expressed as the mean \pm SD of 3 independent experiments.

Immunofluorescence microscopy

Cells were treated with 0.5 μ M SAHA and/or 10 μ M LY for 24 h, seeded on glass coverslips for 15 min, washed with RPMI 1640 to remove debris, allowed to spread for 15 min in RPMI containing 1 ng/ml CXCL12, and fixed with 4% paraformaldehyde. The fixed cells were permeabilized in 0.1% Triton X-100 and blocked in 3% BSA before the addition of the primary antibody (anti- α -tubulin 1:500; Sigma-Aldrich) at 4°C overnight. Cells were then incubated with Alexa Fluor 488-conjugated anti-rabbit secondary antibody (Sigma-Aldrich), Alexa Fluor 546 phalloidin (Invitrogen, Thermo Fisher Scientific), and DAPI for 60 min at room temperature. Coverslips were mounted on glass slides by use of fluorescent mounting medium (Dako), analyzed by use of a Zeiss LSM510 confocal microscope with a 63 \times objective, and processed using Zen software (Zeiss, Thornwood, NY, USA).

qPCR analysis

Total RNA was extracted from cells by use of an RNeasy Mini kit (Qiagen, Valencia, CA, USA), according to the manufacturer's instructions, and was purified by use of a DNase-free kit (Ambion, Life Technologies, Carlsbad, CA, USA) to remove contaminating DNA. The expression of RhoA, -B, and -C; Rac1, -2, and -3; and Rnd1, -2, and -3 was detected via qPCR by use of Brilliant III Ultra-Fast SYBR Green QRT-PCR Master Mix (Agilent Technologies, Santa Clara, CA, USA) and an ABI 7500 Sequence Detection System (PE Applied Biosystems, Foster City, CA, USA) by use of specific primers (see Supplemental information). GAPDH was used as an endogenous control. The relative mRNA levels were calculated as comparative cycle threshold.

Western blotting

Western blot analysis was performed as described previously [12]. The anti-RhoB, -RhoC, and -Cdc42 antibodies were obtained from Santa Cruz Biotechnology (Santa Cruz, CA, USA). The anti-RhoA anti-Akt, anti-phospho-Akt (Ser 473), and anti-phospho-ERK1/2 antibodies were obtained from Cell Signaling Technology (Danvers, MA, USA), and the anti-ERK1/2 antibody was obtained from Invitrogen, Thermo Fisher Scientific. The secondary antibodies HRP-labeled anti-mouse and anti-rabbit were from Amersham Biosciences (Piscataway, NJ, USA).

RhoA activity assay

The RhoA activity assay was performed by use of the RhoA G-LISA Activation Assay Biochem Kit (Cytoskeleton, Denver, CO, USA), according to the manufacturer's instructions. The RhoA G-LISA kit contains the Rho-binding domain from Rhotekin bound to the wells of a 96-well plate. Active GTP-bound Rho in the cell lysates binds to the wells, whereas inactive GDP-bound Rho does not bind. The bound active RhoA is detected by use of a RhoA-specific antibody and chemiluminescence.

Statistical analyses

All data are expressed as the means \pm SD of at least 3 different experiments. The IC₅₀ values were calculated by use of nonlinear regression (curve fit),

and the statistical comparison among groups was performed by use of ANOVA followed by Bonferroni post-test. Statistical significance was set at $P < 0.05$. The analyses were performed by use of GraphPad Prism 5.0 software.

RESULTS

Dose-response curve of SAHA and LY in BL cells

To determine the concentration at which inhibitors were not toxic individually, we established dose response curves to the HDACi SAHA (0–5.0 μM ; Fig. 1, upper) and the PI3Ki LY (0–10.0 μM) at 24, 48, and 72 h (Fig. 1, lower) in the BL cell lines Daudi and Namalwa. Dose-dependent cytotoxicity was observed after 24 h of incubation with the inhibitors (Fig. 1). The final concentrations of SAHA (0.5 μM) and LY (5 μM) and an incubation time of 48 h were selected to evaluate the combination therapy, as they are not cytotoxic separately. The IC_{50} value for Daudi cells, when treated with SAHA for 48 h, was 6.3 μM and when treated with LY, was 12.4 μM . For Namalwa cells, the IC_{50} value when treated with SAHA was 1.36 μM and with LY, was 13.6 μM .

An HDACi potentiates the cell viability inhibition and cell cycle arrest induced by a PI3Ki

We first evaluated the effects of the SAHA/LY combination on cell viability inhibition by use of a Trypan blue exclusion assay. This combination synergistically decreased cell viability after 48 h of treatment in Namalwa ($R = 0.79$) and Daudi cells ($R = 0.69$), reaching ~50% viability inhibition (single treatment vs. combined treatment; Fig. 2). To evaluate the growth inhibitory effects of the inhibitors, we investigated the DNA content distribution in Namalwa and Daudi cells. The HDACi SAHA at

0.5 μM did not induce cell cycle arrest, but 5 μM LY arrested cells in the G0/G1 phase. The combination of SAHA and LY enhanced G0/G1 arrest and concomitantly decreased the percentage of cells in the S phase (Fig. 3). These results suggest that the SAHA/LY combination inhibits the proliferation of Namalwa and Daudi cell lines.

PI3Ki suppresses Akt and ERK phosphorylation

The PI3Ki LY inhibits PI3K and hence, activation of its downstream targets, such as Akt and ERK1/2, both of which contribute to cell growth and proliferation [13]. To evaluate the ability of an HDACi combined with a PI3Ki to suppress the phosphorylation and activation of downstream kinases involved in cell growth and proliferation, we evaluated the Akt and ERK1/2 phosphorylation levels in Namalwa and Daudi cells after SAHA and LY treatment. We observed a decrease in Akt and ERK1/2 phosphorylation following treatment with the LY and SAHA/LY combination (Fig. 4A and B). In addition, the effect of LY on Akt phosphorylation in Daudi cells was less effective compared with Namalwa cells, probably as a result of a mutation in the exon 6 of the phosphoinositide phosphatase *PTEN* gene (t524g/v175G) [14]. Loss of the PTEN tumor suppressor gene leads to an increase in the phosphoinositide products of PI3K and hence, Akt activation and has been reported in many cancers, including B-NHL [15].

Cotreatment with an HDACi and a PI3Ki suppresses BL cell migration

PI3K is known to regulate cell migration as well as cell survival and growth [13]. Therefore, we evaluated whether SAHA and LY, individually or in combination, affect BL cell migration. After treatment of Namalwa cells for 24 h, each inhibitor alone and in combination inhibited cell migration in an additive manner

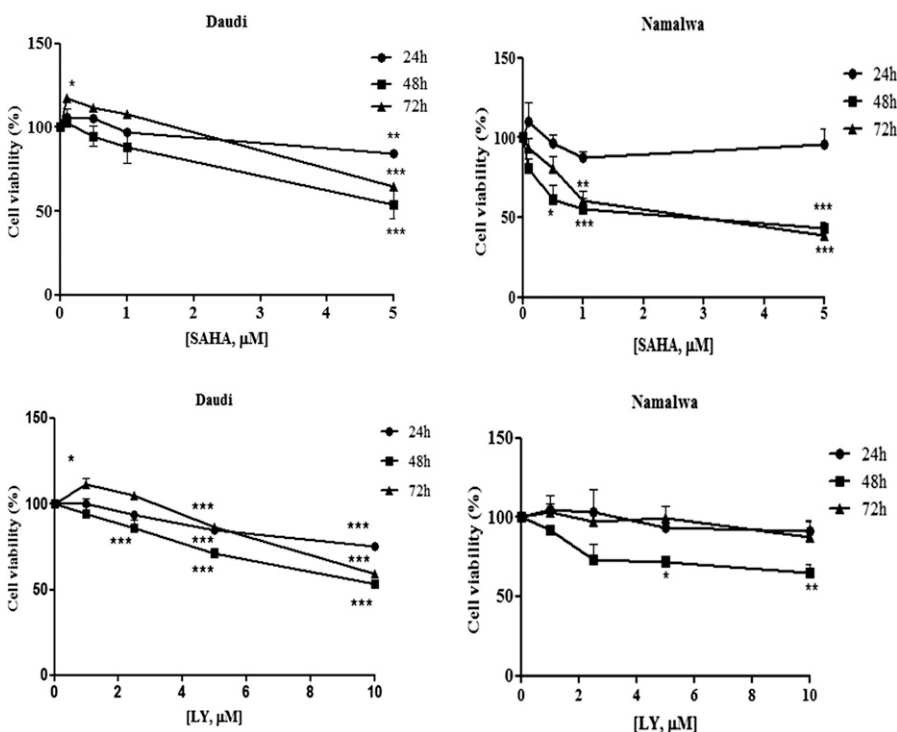


Figure 1. HDACi and PI3Ki reduce BL cell viability. Daudi and Namalwa cell lines were treated with 0.1–5 μM SAHA (upper graphs) or 1.0–10 μM LY (lower graphs), and cell viability was evaluated by MTT assay. Data are means \pm sd of 3 independent experiments and are shown as percent of untreated cells. Significance vs. untreated cells; * $P < 0.05$; ** $P < 0.01$; *** $P < 0.001$.

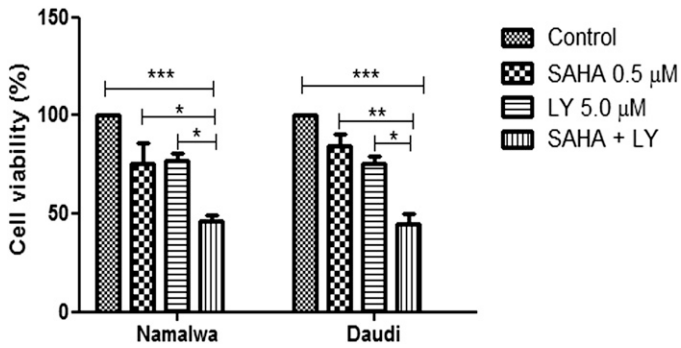


Figure 2. Viability inhibition by HDACi and PI3Ki in BL cell lines. Daudi and Namalwa cell lines were treated with 0.5 μ M SAHA and/or 5.0 μ M LY for 48 h. Viability was determined by Trypan blue exclusion assay. Data are means \pm SD of 3 independent experiments, shown relative to control. Control, Cells treated with vehicle (DMSO). Significance vs. untreated cells; * P < 0.05; ** P < 0.01; *** P < 0.001.

($R = 1.2$). To confirm the involvement of the PI3K pathway in cell migration, we treated Namalwa cells with a selective inhibitor of PI3K δ (PI3K δ inhibitor X, IC87114; Calbiochem, EMD Millipore, Billerica, MA, USA), as LY inhibits the protein kinase mTOR as well as PI3Ks [16]. The PI3K family comprises 3 subgroups: class I (IA and IB), class II, and class III. Class IA is activated by Ras signaling and consists of 3 catalytic isoforms: p110 α , p110 β , and p110 δ , of which p110 δ negatively controls RhoA and PTEN and is most abundant in leukocytes [4, 17]. The PI3K δ inhibitor X alone decreased Namalwa cell migration similarly to LY, and the SAHA/PI3K δ inhibitor X combination decreased cell migration to the same extent as SAHA/LY (Fig. 5). This indicates that the effect of LY is likely to be primarily a result of inhibiting PI3K δ rather than mTOR or other PI3Ks.

The inhibition of cell migration by PI3Ki and HDACi is associated with decreased cell polarization

To determine whether the effects of PI3Ki and HDACi on cell migration were a result of altered cell shape or cytoskeletal organization, we examined F-actin and α -tubulin localization in Namalwa cells after 24 h of SAHA and LY treatment to avoid cell death induction (Fig. 6A). We counted the percent of polarized cells, defined by the highest level of tubulin at the front and F-actin at the rear of the cells. Treatment with SAHA and LY together decreased the percent of polarized cells compared with either treatment alone (Fig. 6B). This effect correlated with increased α -tubulin acetylation, which is an HDAC6 target and regulates the stability of microtubules [18]. However, the decrease in cell polarity was not correlated with Cdc42 levels (Fig. 6C), which is known to be important for migratory cell polarity [19]. We also observed that SAHA induced a less round and compact morphology (Fig. 6A). Therefore, we analyzed the cell area and roundness and observed a decrease in cell area but not roundness after SAHA or LY treatment (Supplemental Fig. 1). However, combined SAHA/LY treatment did not significantly decrease cell area, possibly because each inhibitor acts through a different mechanism to affect cell area.

An HDACi and a PI3Ki alter Rho GTPase expression

To elucidate the mechanisms involved in the inhibition of cell migration by SAHA and LY, we performed qPCR to measure the mRNA levels of RhoA, RhoB, and RhoC, which are known to regulate cell migration [20], after treatment of Namalwa cells. Both inhibitors enhanced the expression of RhoB and RhoC but not RhoA. However, there is no additive effect when both inhibitors are used together (Fig. 7A). Surprisingly, there was no change in RhoC protein expression (Fig. 7B), despite the strong increase in RhoC mRNA levels. However, SAHA enhanced RhoB protein levels (Fig. 7C). Interestingly, LY and SAHA affected RhoA activity (Fig. 7C). LY increased RhoA activity, consistent with the known inverse correlation between PI3K/Rac activity and RhoA activity. In contrast, SAHA reduced RhoA activity, possibly because it alters the expression of a Rho-guanine nucleotide exchange factor or Rho-GTPase-activating protein.

DISCUSSION

Although new treatment strategies that use intensive regimes of chemotherapy are very successful for pediatric BL treatment, resulting in high cure rates (80–95%) [21, 22], some patients are diagnosed at disease stage IV, representing the dissemination of BL into the BM and/or the CNS, which is associated with poor prognosis and a significant risk of treatment failure. The 4-yr survival rate of pediatric patients with progressive or recurrent disease is ~16% [5, 23, 24]. At least 30% of BL cases occur in patients older than 60 yr, and the absolute number of BL cases in adults is higher than that in children. In adults, as in children, CNS and BM involvement and poor general status are associated with poor prognosis of BL [25].

To improve the BL treatment response in specific groups of patients, further understanding of the molecular biology of this disease is necessary. Our group has shown the promising potential of a combination therapy consisting of an HDACi and chemotherapy for BL cells [12]. We observed a synergistic effect of the sodium butyrate/etoposide combination and noted the involvement of PI3K signaling in the treatment response [7]. Recent clinical studies (phases I and III), with striking results, provided robust evidence that the PI3K δ inhibitor CAL-101 (idelalisib), a potent, selective inhibitor of p110 δ , has high efficacy and acceptable safety profile in patients with CLL, indolent B-NHL, and relapsed/refractory mantle cell lymphoma [26–29]. On the basis of these studies, idelalisib was the first PI3Ki approved by regulatory agencies for treatment of CLL and refractory indolent B cell lymphomas [30]. Although idelalisib shows activity as a single agent, it may be more effective when combined with other drugs, as has been demonstrated in several clinical trials [31].

Remarkably, the combined treatment with a PI3Ki/mTOR inhibitor and a pan-HDACi exhibits potent preclinical activity in vitro and in vivo in DLBCL and other types of B-NHL. In contrast, this combination has little toxicity toward normal hematopoietic CD34⁺ cells, suggesting a possible therapeutic

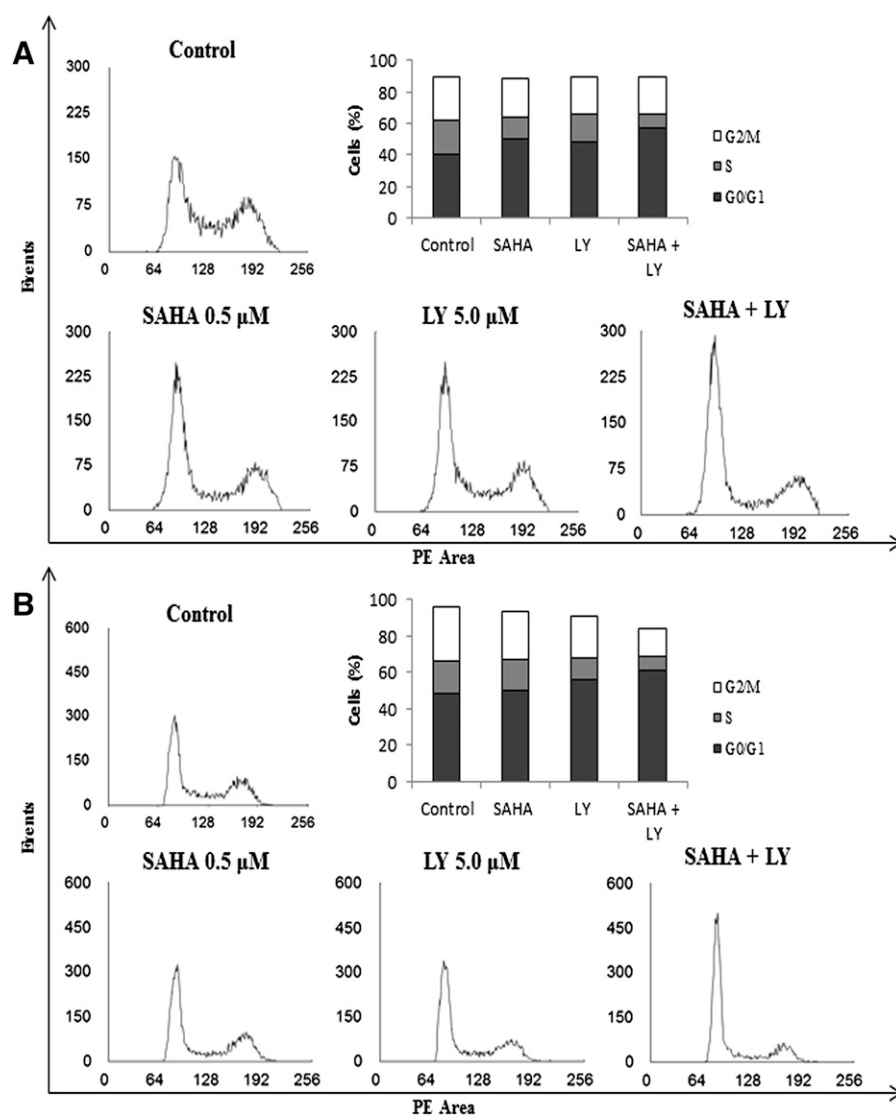


Figure 3. HDACi and PI3Ki induce cell cycle arrest. Namalwa (A) and Daudi (B) cells were treated with 0.5 μ M SAHA and/or 5.0 μ M LY for 48 h and DNA content was evaluated by flow cytometry. One representative of 3 independent experiments is shown.

selectivity for NHL cells [32]. Therefore, the combination of PI3Ki and HDACi may be a valuable and effective strategy for treatment of some B-NHL that present with PI3K/Akt activation, including BL [3, 33].

Recently, the therapeutic targeting of PI3K in BL has been suggested, based on the cooperation between PI3K and MYC during BL pathogenesis [2, 3]. Here, we evaluated the effects of the HDACi SAHA combined with the PI3Ki LY on BL cell growth and migration.

The combination of SAHA and LY at low doses enhanced the effects of each compound alone in inhibiting cell viability and proliferation and inducing cell cycle arrest. These results corroborate studies that have demonstrated the effectiveness of such combinations on other types of cancer, such as relapsed/refractory ALL [34], endometrial carcinoma [35], renal cell carcinoma [36], and head and neck squamous cell carcinoma [37]. Recently, Burke et al. [34] showed that reinduction chemotherapy after decitabine, a well-known demethylating agent, and SAHA treatment

provided benefits in the treatment of relapsed lymphoblastic leukemia (ALL) patients; the response of these patients to this treatment could be validated based on their methylation status. On the other hand, whereas most patients with B-NHL showed no response to HDACi monotherapy, these drugs might be more effective if they are combined with other therapeutic agents [38–40]. A phase II study examined the activity and tolerability of SAHA and the CD20 antibody rituximab in patients with relapsed/refractory follicular, marginal zone, and mantle cell lymphoma. The combination of SAHA and rituximab was effective and displayed an acceptable safety profile and sustained responses, emphasizing that the combinatorial approach that uses epigenetic modifiers and targeted therapy could be promising in treatment of relapse/refractory patients with leukemia or lymphoma [41]. Other results support a potential role of HDACi in combination therapy for overcoming treatment resistance in DLBCL. The combination of the chemotherapeutic agent bendamustine with the HDACi vorinostat (SAHA) enhanced histone acetylation and

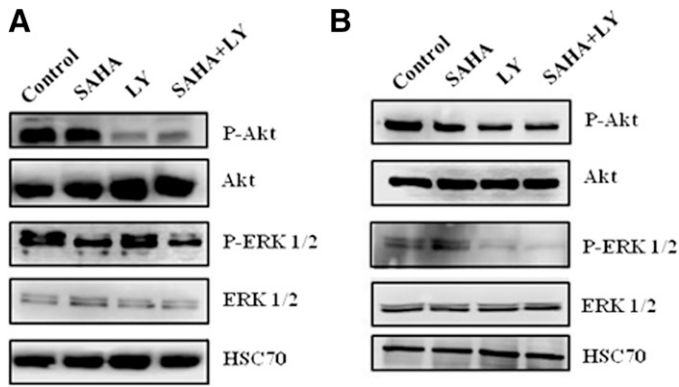


Figure 4. Effect of HDACi and PI3Ki on PI3K-dependent signaling. Namalwa (A) and Daudi (B) BL cell lines were treated with 0.5 μ M SAHA and/or 5.0 μ M LY. Protein levels were determined by use of the indicated antibodies by Western blotting. Heat-shock cognate 70 (HSC70) was used as a loading control. One representative of 3 independent experiments is shown. P, Phosphorylation.

dsDNA breaks, resulting in an additive to synergistic cytotoxic effect in activated B cell- and germinal center B cell-type DLBCL cells [42]. In addition, combined PI3Ki/HDACi enhanced cell death in several DLBCL lines, including poor prognosis subtypes, and exhibited potent activity in a murine xenograft model [32].

The inhibition of PI3K/Akt and ERK1/2 has been reported to reduce cell migration and induce cell death in solid tumors, such as small cell lung cancer, hepatoma, and NHL [43–45]. Most BL cell lines have constitutively high levels of PI3K activity. Previously, the analysis of BL cell lines showed high levels of phospho-Akt, which were reduced by treatment with the PI3Ki LY [3]. Our observations agree with these findings; we observed a reduction in Akt and ERK1/2 phosphorylation upon treatment with SAHA and LY in 2 BL cell lines.

BL progression and dissemination into BM and CNS are likely to involve cell migration. We find that the SAHA/LY combination strongly inhibits the migration of BL cells, independently of mTOR signaling. Cytoskeletal dynamics are crucial for cell polarity and migration, and the Rho GTPase family of proteins is a key coordinator of cell migration [46]. In particular, Cdc42 play a central role in establishing cell polarity in all eukaryotic cells, irrespective of the biologic context [19]. Cdc42 is also essential for B-lymphocyte development and activation. Deletion of Cdc42 in mice from the pro-/pre-B cell stage significantly blocked B cell development and reduced mature B cell populations [47]. We did not observe any alteration in Cdc42 expression after treatment with an HDACi and/or a PI3Ki; however, the disruption of cell polarity may be related to alterations in the activity or localization of Cdc42 and/or expression of Cdc42 effectors, such as WASP [48] or Par6 [49].

HDACi affect the transcription of multiple genes, and their effects on gene expression are complex [50]. In addition to regulating histone modification, HDACs regulate the acetylation status of nonhistone proteins that regulate the cellular cytoskeleton, such as α -tubulin [18]. The acetylation

of α -tubulin is mediated by HDAC6, a well-known regulator of cell motility [51], which is a target of the pan-HDACi SAHA [18]. The inhibition of HDAC6 leads to an enhancement of α -tubulin acetylation, which we also observed here following SAHA treatment. In a recent report, inhibition of HDAC6 activity by use of HDACi and small interfering RNA suppressed the motility of Raji cells, a BL cell line [52]. Thus, the notion of targeting HDAC6 by use of isoform-specific molecules is attracting interest. Inhibition of HDAC6 increases the effectiveness of the chemotherapeutic agent etoposide, doxorubicin, and SAHA in transformed human prostate cancer but not in normal fibroblast cells [53]. Another SAHA target is HDAC1, which is involved in the repression of RhoB expression. RhoB is thought to be a tumor suppressor, and HDAC1 inhibition enhanced RhoB levels, suggesting a potential therapeutic benefit of HDACi for NSCLC [54]. We also observed an increase in the mRNA levels of RhoB and RhoC after HDACi and PI3Ki treatment. We hypothesize that the enhancement of Rho gene expression may be an indirect effect of PI3Ki, as increased mRNA levels of other Rho members, such as Rac1, -2, and -3 and Rnd1, -2, and -3, were also observed (data not shown). LY abrogates the phosphorylation of Akt, which in turn, enhances the expression of the transcription factor FOXO1 and FOXO3 [55]. FOXOs stimulate the expression of a broad spectrum of genes, and we hypothesize that these could include Rho family members. However, few studies, so far, have suggested cross-talk

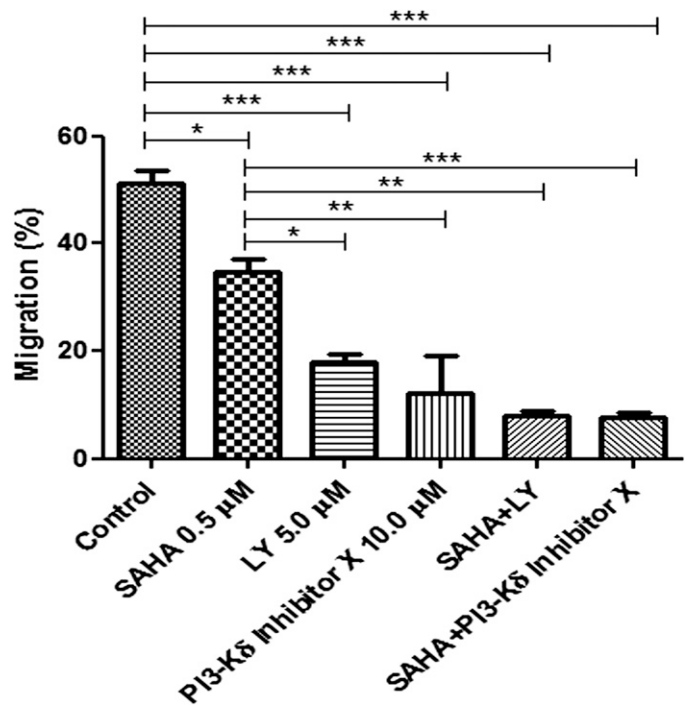


Figure 5. PI3Ki and HDACi reduce migration of BL cells. Cells were allowed to migrate for 24 h in the presence of 100 ng/ml CXCL12 in the lower chamber of transwell plates and the inhibitors as indicated. Graph shows the mean \pm sd of 3 independent experiments; * P < 0.05; ** P < 0.01; *** P < 0.001.

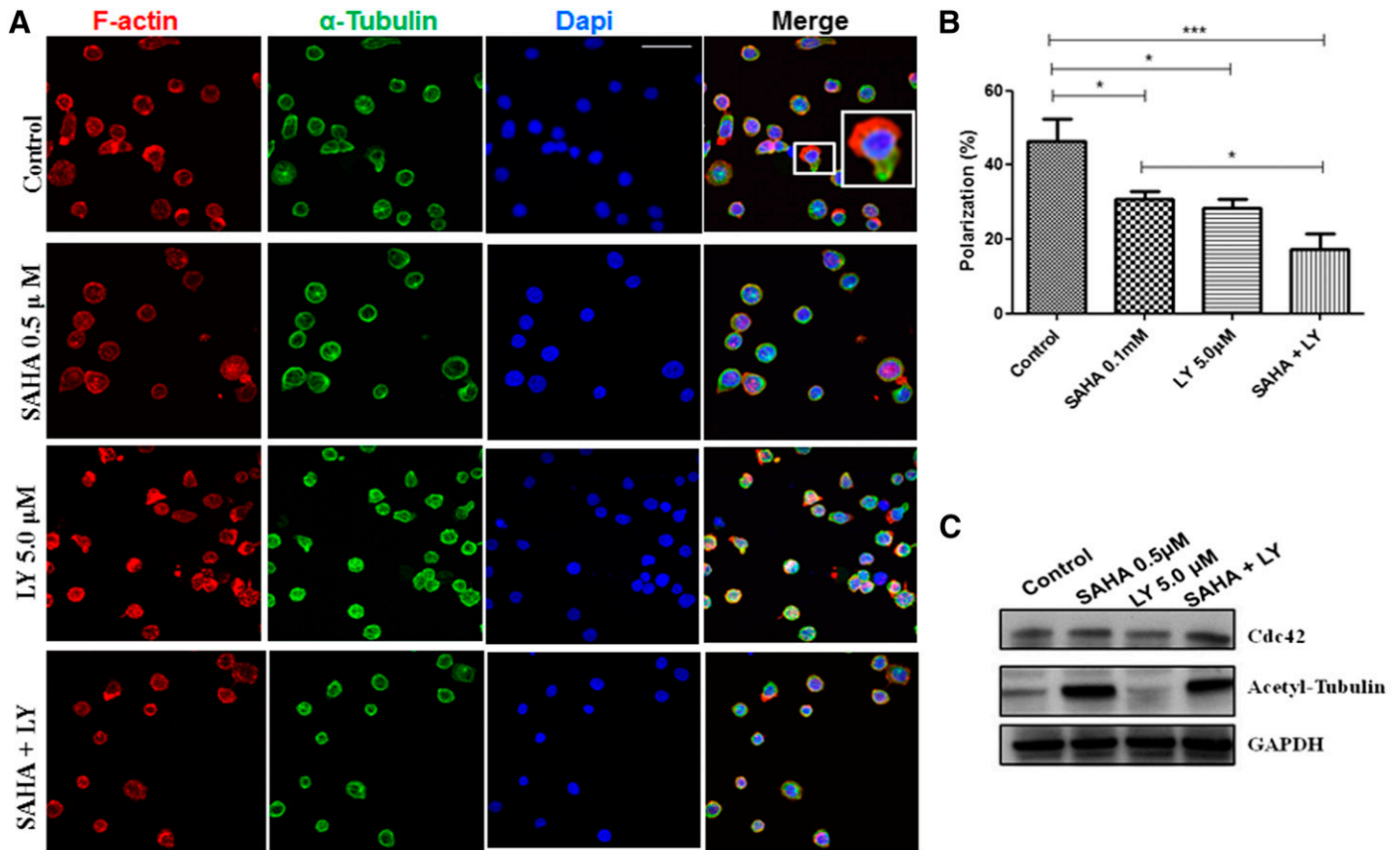


Figure 6. PI3Ki and HDACi alter BL cell shape. Namalwa cells were treated with SAHA and/or LY for 24 h. (A) Cells were fixed and stained for F-actin (Phalloidin, red), α -tubulin (green), and DNA (DAPI, blue). Zoom shows a typical polarized cell. Original scale bar, 10 μ m. (B) The polarized cells were counted. At least 300 cells were counted in each of 3 experiments. Graph shows mean \pm SD of 3 independent experiments; * $P < 0.05$; *** $P < 0.001$. (C) Cdc42 levels and α -tubulin acetylation were assessed by Western blotting.

between FOXO signaling and Rho expression. Previously, we found that HDACi potentiate chemotherapy-induced apoptosis via the up-regulation of Bim [12], a transcriptional target of FOXO3 [56].

Although we described alterations in Rho gene expression after treatment of BL cells with an HDACi and/or a PI3Ki, we did not detect an association between the mRNA and protein levels of RhoA or RhoC but did for RhoB. However, RhoA activity was affected by SAHA and LY. It has recently been reported that *RhoA* is mutated in 8.5% of pediatric BL patients, and the mutations are predicted to prevent activation of RhoA [57]. In addition, the expression of Rho GTPases may be regulated by miRs. For example, RhoC mRNA is a target of miR-493 and miR-138, which are involved in the reduction of cancer cell migration [20]. The suppression of miR-131 has also been reported to increase RhoA expression in a human breast cancer cell model [20]. In a pancreatic cancer model, miR-143 expression significantly inhibited pancreatic cancer cell migration and invasion, liver metastasis, and xenograft tumor growth in vivo [58]. Notably, our group has reported the loss of miR-143 expression in 46 pediatric BL samples, but at present, it is unclear how miR-143 contributes to BL pathogenesis [7].

We observed an increase in RhoB mRNA and protein levels after HDACi treatment, and these effects were associated with a decrease in cell migration. The loss of RhoB expression has been reported in several cancer cell types and has been associated with increased cell migration and reduced apoptosis [59–61]. Thus, RhoB is postulated to be a tumor suppressor gene that is repressed by HDAC1 [54]. A trend toward poor prognosis in NSCLC patients has been associated with no or low expression of RhoB. Moreover, RhoB expression in NSCLC cell lines was induced via HDACi, suggesting that histone modification may contribute to RhoB down-regulation [62]. RhoB function has also been linked to the regulation of PI3K/Akt survival pathways [63]. In tumor cells, the regulation of the Akt signaling pathway by RhoB controls cell invasion and migration [64]. Additionally, during breast cancer development, RhoB loss increases tumor initiation and tumor cell growth [65]. These reports reinforce our observations and suggest cross-talk between RhoB and the PI3K/Akt pathway in BL biology.

In summary, we demonstrate that the combination of an HDACi and a PI3Ki inhibited both cell proliferation and migration, potentially via alterations in PI3K signaling and HDAC function, which regulates α -tubulin

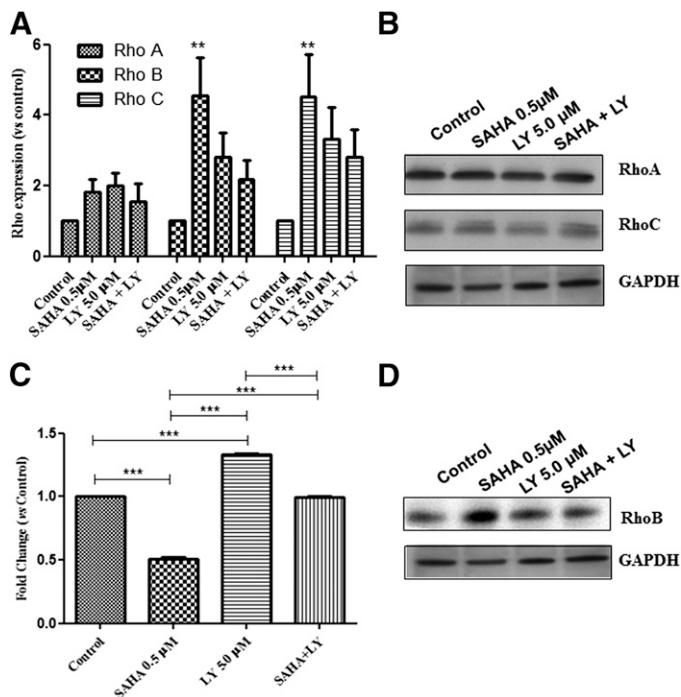


Figure 7. PI3Ki and HDACi affect Rho family expression and activity. Namalwa cells were treated with SAHA and/or LY for 24 h, and the mRNA levels of RhoA, RhoB, and RhoC were determined by qPCR (A). RhoA and RhoC (B) and RhoB (D) protein levels were assessed by Western blotting and RhoA activity by G-LISA assay (C). Graph shows mean \pm SD of 3 independent experiments; ** $P < 0.01$; *** $P < 0.001$ relative to control cells.

acetylation and RhoB expression. These data suggest that a combinatorial approach complementing existing chemotherapy strategies is promising for BL treatment.

AUTHORSHIP

A.C.S.F. designed and performed the experiments, interpreted the results, and wrote the manuscript. J.C.M.D.F.J. and J.A.M.D. analyzed the data and revised the manuscript. A.J.R. designed the migration assays, provided laboratory support for research, and critically revised the manuscript. C.E.K. analyzed the data, provided relevant clinical setting content, and wrote the manuscript. All of the authors approved the final manuscript.

ACKNOWLEDGMENTS

This work was supported by grants from Instituto Nacional de Ciência e Tecnologia (INCT) para Controle do Câncer: National Council for Scientific and Technological Development (CNPq) 573806/2008-0/Fundação Carlos Chagas Filho de Amparo à Pesquisa do Estado do Rio de Janeiro (FAPERJ) E26/170.026/2008; Programa de Oncobiologia/Fundação do Câncer, FAPERJ E-26/110.375/2014; and Cancer Research UK C6220/15961 (to A.J.R.). A.C.S.F. had a scholarship from Ministério da Saúde/Instituto Nacional de Câncer (INCA) and Ministério da

Educação/Coordenação de Aperfeiçoamento de Pessoal de Nível Superior-Programa de Doutorado Sanduíche no Exterior (CAPES-PDSE).

DISCLOSURES

The authors declare no conflicts of interest.

REFERENCES

- Klappproth, K., Wirth, T. (2010) Advances in the understanding of MYC-induced lymphomagenesis. *Br. J. Haematol.* **149**, 484–497.
- Sander, S., Calado, D. P., Srinivasan, L., Köchert, K., Zhang, B., Rosolowski, M., Rodig, S. J., Holzmann, K., Stilgenbauer, S., Siebert, R., Bullinger, L., Rajewsky, K. (2012) Synergy between PI3K signaling and MYC in Burkitt lymphomagenesis. *Cancer Cell* **22**, 167–179.
- Schmitz, R., Young, R. M., Ceribelli, M., Jhavar, S., Xiao, W., Zhang, M., Wright, G., Shaffer, A. L., Hodson, D. J., Buras, E., Liu, X., Powell, J., Yang, Y., Xu, W., Zhao, H., Kohlhammer, H., Rosenwald, A., Kluin, P., Müller-Hermelink, H. K., Ott, G., Gascoyne, R. D., Connors, J. M., Rimsza, L. M., Campo, E., Jaffe, E. S., Delabie, J., Smeland, E. B., Olgwang, M. D., Reynolds, S. J., Fisher, R. I., Braziel, R. M., Tubbs, R. R., Cook, J. R., Weisenburger, D. D., Chan, W. C., Pittaluga, S., Wilson, W., Waldmann, T. A., Rowe, M., Mbulaitete, S. M., Rickinson, A. B., Staudt, L. M. (2012) Burkitt lymphoma pathogenesis and therapeutic targets from structural and functional genomics. *Nature* **490**, 116–120.
- Cain, R. J., Ridley, A. J. (2009) Phosphoinositide 3-kinases in cell migration. *Biol. Cell* **101**, 13–29.
- Cairo, M. S., Spoto, R., Gerrard, M., Auperin, A., Goldman, S. C., Harrison, L., Pinkerton, R., Raphael, M., McCarthy, K., Perkins, S. L., Patte, C. (2012) Advanced stage, increased lactate dehydrogenase, and primary site, but not adolescent age (≥ 15 years), are associated with an increased risk of treatment failure in children and adolescents with mature B-cell non-Hodgkin's lymphoma: results of the FAB LMB 96 study. *J. Clin. Oncol.* **30**, 387–393.
- Sander, S., Rajewsky, K. (2012) Burkitt lymphomagenesis linked to MYC plus PI3K in germinal center B cells. *Oncotarget* **3**, 1066–1067.
- Ferreira, A. C., Robaina, M. C., Rezende, L. M., Severino, P., Klumb, C. E. (2014) Histone deacetylase inhibitor prevents cell growth in Burkitt's lymphoma by regulating PI3K/Akt pathways and leads to upregulation of miR-143, miR-145, and miR-101. *Ann. Hematol.* **93**, 983–993.
- Richon, V. M., Zhou, X., Rifkind, R. A., Marks, P. A. (2001) Histone deacetylase inhibitors: development of suberoylanilide hydroxamic acid (SAHA) for the treatment of cancers. *Blood Cells Mol. Dis.* **27**, 260–264.
- Fischel, J. L., Formento, P., Milano, G. (2005) Epidermal growth factor receptor double targeting by a tyrosine kinase inhibitor (Iressa) and a monoclonal antibody (Cetuximab). Impact on cell growth and molecular factors. *Br. J. Cancer* **92**, 1063–1068.
- Chou, T. C., Talalay, P. (1984) Quantitative analysis of dose-effect relationships: the combined effects of multiple drugs or enzyme inhibitors. *Adv. Enzyme Regul.* **22**, 27–55.
- Favaro, P., Traina, F., Machado-Neto, J. A., Lazarini, M., Lopes, M. R., Pereira, J. K., Costa, F. F., Infante, E., Ridley, A. J., Saad, S. T. (2013) FMNL1 promotes proliferation and migration of leukemia cells. *J. Leukoc. Biol.* **94**, 503–512.
- Dos Santos Ferreira, A. C., Fernandes, R. A., Kwee, J. K., Klumb, C. E. (2012) Histone deacetylase inhibitor potentiates chemotherapy-induced apoptosis through Bim upregulation in Burkitt's lymphoma cells. *J. Cancer Res. Clin. Oncol.* **138**, 317–325.
- Rosich, L., Montraveta, A., Xargay-Torrent, S., López-Guerra, M., Roldán, J., Aymerich, M., Salaverria, I., Beà, S., Campo, E., Pérez-Galán, P., Roué, G., Colomer, D. (2014) Dual PI3K/mTOR inhibition is required to effectively impair microenvironment survival signals in mantle cell lymphoma. *Oncotarget* **5**, 6788–6800.
- Boulanger, E., Marchio, A., Hong, S. S., Pineau, P. (2009) Mutational analysis of TP53, PTEN, PIK3CA and CTNNB1/beta-catenin genes in human herpesvirus 8-associated primary effusion lymphoma. *Haematologica* **94**, 1170–1174.
- Abubaker, J., Bavi, P. P., Al-Harbi, S., Siraj, A. K., Al-Dayel, F., Uddin, S., Al-Kuraya, K. (2007) PIK3CA mutations are mutually exclusive with PTEN loss in diffuse large B-cell lymphoma. *Leukemia* **21**, 2368–2370.
- Brunn, G. J., Williams, J., Sabers, C., Wiederrecht, G., Lawrence, Jr., J. C., Abraham, R. T. (1996) Direct inhibition of the signaling functions of the mammalian target of rapamycin by the phosphoinositide 3-kinase inhibitors, wortmannin and LY294002. *EMBO J.* **15**, 5256–5267.

17. Papakonstanti, E. A., Ridley, A. J., Vanhaesebroeck, B. (2007) The p110delta isoform of PI 3-kinase negatively controls RhoA and PTEN. *EMBO J.* **26**, 3050–3061.
18. Chun, P. (2015) Histone deacetylase inhibitors in hematological malignancies and solid tumors. *Arch. Pharm. Res.* **38**, 933–949.
19. Etienne-Manneville, S. (2004) Cdc42—the centre of polarity. *J. Cell Sci.* **117**, 1291–1300.
20. Ridley, A. J. (2013) RhoA, RhoB and RhoC have different roles in cancer cell migration. *J. Microsc.* **251**, 242–249.
21. Reiter, A., Schrappe, M., Tiemann, M., Ludwig, W. D., Yakisan, E., Zimmermann, M., Mann, G., Chott, A., Ebell, W., Klingebiel, T., Graf, N., Kremens, B., Müller-Weihrich, S., Plüss, H. J., Zintl, F., Henze, G., Riehm, H. (1999) Improved treatment results in childhood B-cell neoplasms with tailored intensification of therapy: a report of the Berlin-Frankfurt-Münster Group Trial NHL-BFM 90. *Blood* **94**, 3294–3306.
22. Patte, C., Auperin, A., Gerrard, M., Michon, J., Pinkerton, R., Spoto, R., Weston, C., Raphael, M., Perkins, S. L., McCarthy, K., Cairo, M. S.; FAB/LMB96 International Study Committee. (2007) Results of the randomized international FAB/LMB96 trial for intermediate risk B-cell non-Hodgkin lymphoma in children and adolescents: it is possible to reduce treatment for the early responding patients. *Blood* **109**, 2773–2780.
23. Griffin, T. C., Weitzman, S., Weinstein, H., Chang, M., Cairo, M., Hutchison, R., Shiramizu, B., Wiley, J., Woods, D., Barnich, M., Gross, T. G.; Children's Oncology Group. (2009) A study of rituximab and ifosfamide, carboplatin, and etoposide chemotherapy in children with recurrent/refractory B-cell (CD20+) non-Hodgkin lymphoma and mature B-cell acute lymphoblastic leukemia: a report from the Children's Oncology Group. *Pediatr. Blood Cancer* **52**, 177–181.
24. Cairo, M. S., Gerrard, M., Spoto, R., Auperin, A., Pinkerton, C. R., Michon, J., Weston, C., Perkins, S. L., Raphael, M., McCarthy, K., Patte, C.; FAB LMB96 International Study Committee. (2007) Results of a randomized international study of high-risk central nervous system B non-Hodgkin lymphoma and B acute lymphoblastic leukemia in children and adolescents. *Blood* **109**, 2736–2743.
25. Ribera, J. M., García, O., Grande, C., Esteve, J., Oriol, A., Bergua, J., González-Campos, J., Vall-Llovera, F., Tormo, M., Hernández-Rivas, J. M., García, D., Brunet, S., Alonso, N., Barba, P., Miralles, P., Llorente, A., Montesinos, P., Moreno, M. J., Hernández-Rivas, J. A., Bernal, T. (2013) Dose-intensive chemotherapy including rituximab in Burkitt's leukemia or lymphoma regardless of human immunodeficiency virus infection status: final results of a phase 2 study (Burkimab). *Cancer* **119**, 1660–1668.
26. Brown, J. R., Byrd, J. C., Coutre, S. E., Benson, D. M., Flinn, I. W., Wagner-Johnston, N. D., Spurgeon, S. E., Kahl, B. S., Bello, C., Webb, H. K., Johnson, D. M., Peterman, S., Li, D., Jahn, T. M., Lannutti, B. J., Ulrich, R. G., Yu, A. S., Miller, L. L., Furman, R. R. (2014) Idelalisib, an inhibitor of phosphatidylinositol 3-kinase p110δ, for relapsed/refractory chronic lymphocytic leukemia. *Blood* **123**, 3390–3397.
27. Furman, R. R., Sharman, J. P., Coutre, S. E., Cheson, B. D., Pagel, J. M., Hillmen, P., Barrientos, J. C., Zelenetz, A. D., Kipps, T. J., Flinn, I., Ghia, P., Eradat, H., Ervin, T., Lamanna, N., Coiffier, B., Pettitt, A. R., Ma, S., Stilgenbauer, S., Cramer, P., Aiello, M., Johnson, D. M., Miller, L. L., Li, D., Jahn, T. M., Dansey, R. D., Hallek, M., O'Brien, S. M. (2014) Idelalisib and rituximab in relapsed chronic lymphocytic leukemia. *N. Engl. J. Med.* **370**, 997–1007.
28. Flinn, I. W., Kahl, B. S., Leonard, J. P., Furman, R. R., Brown, J. R., Byrd, J. C., Wagner-Johnston, N. D., Coutre, S. E., Benson, D. M., Peterman, S., Cho, Y., Webb, H. K., Johnson, D. M., Yu, A. S., Ulrich, R. G., Godfrey, W. R., Miller, L. L., Spurgeon, S. E. (2014) Idelalisib, a selective inhibitor of phosphatidylinositol 3-kinase-δ, as therapy for previously treated indolent non-Hodgkin lymphoma. *Blood* **123**, 3406–3413.
29. Kahl, B. S., Spurgeon, S. E., Furman, R. R., Flinn, I. W., Coutre, S. E., Brown, J. R., Benson, D. M., Byrd, J. C., Peterman, S., Cho, Y., Yu, A., Godfrey, W. R., Wagner-Johnston, N. D. (2014) A phase 1 study of the PI3Kδ inhibitor idelalisib in patients with relapsed/refractory mantle cell lymphoma (MCL). *Blood* **123**, 3398–3405.
30. Yang, Q., Modi, P., Newcomb, T., Queva, C., Gandhi, V. (2015) Idelalisib: first-in-class PI3K delta inhibitor for the treatment of chronic lymphocytic leukemia, small lymphocytic leukemia, and follicular lymphoma. *Clin. Cancer Res.* **21**, 1537–1542.
31. Curran, E., Smith, S. M. (2014) Phosphoinositide 3-kinase inhibitors in lymphoma. *Curr. Opin. Oncol.* **26**, 469–475.
32. Rahmani, M., Aust, M. M., Benson, E. C., Wallace, L., Friedberg, J., Grant, S. (2014) PI3K/mTOR inhibition markedly potentiates HDAC inhibitor activity in NHL cells through BIM- and MCL-1-dependent mechanisms in vitro and in vivo. *Clin. Cancer Res.* **20**, 4849–4860.
33. Pfeifer, M., Grau, M., Lenze, D., Wenzel, S. S., Wolf, A., Wollert-Wulf, B., Dietze, K., Nogai, H., Storek, B., Madle, H., Dörken, B., Janz, M., Dirnhofer, S., Lenz, P., Hummel, M., Tzankov, A., Lenz, G. (2013) PTEN loss defines a PI3K/AKT pathway-dependent germinal center subtype of diffuse large B-cell lymphoma. *Proc. Natl. Acad. Sci. USA* **110**, 12420–12425.
34. Burke, M. J., Lamba, J. K., Pounds, S., Cao, X., Ghodke-Puranik, Y., Lindgren, B. R., Weigel, B. J., Verneris, M. R., Miller, J. S. (2014) A therapeutic trial of decitabine and vorinostat in combination with chemotherapy for relapsed/refractory acute lymphoblastic leukemia. *Am. J. Hematol.* **89**, 889–895.
35. Yoshioka, T., Yogosawa, S., Yamada, T., Kitawaki, J., Sakai, T. (2013) Combination of a novel HDAC inhibitor OBP-801/YM753 and a PI3K inhibitor LY294002 synergistically induces apoptosis in human endometrial carcinoma cells due to increase of Bim with accumulation of ROS. *Gynecol. Oncol.* **129**, 425–432.
36. Yamada, T., Horinaka, M., Shinnoh, M., Yoshioka, T., Miki, T., Sakai, T. (2013) A novel HDAC inhibitor OBP-801 and a PI3K inhibitor LY294002 synergistically induce apoptosis via the suppression of survivin and XIAP in renal cell carcinoma. *Int. J. Oncol.* **43**, 1080–1086.
37. Erlich, R. B., Kherrouche, Z., Rickwood, D., Endo-Munoz, L., Cameron, S., Dahler, A., Hazar-Rethinam, M., de Long, L. M., Wooley, K., Guminski, A., Saunders, N. A. (2012) Preclinical evaluation of dual PI3K-mTOR inhibitors and histone deacetylase inhibitors in head and neck squamous cell carcinoma. *Br. J. Cancer* **106**, 107–115.
38. O'Connor, O. A., Heaney, M. L., Schwartz, L., Richardson, S., Willim, R., MacGregor-Cortelli, B., Curly, T., Moskowitz, C., Portlock, C., Horwitz, S., Zelenetz, A. D., Frankel, S., Richon, V., Marks, P., Kelly, W. K. (2006) Clinical experience with intravenous and oral formulations of the novel histone deacetylase inhibitor suberoylanilide hydroxamic acid in patients with advanced hematologic malignancies. *J. Clin. Oncol.* **24**, 166–173.
39. Crump, M., Coiffier, B., Jacobsen, E. D., Sun, L., Ricker, J. L., Xie, H., Frankel, S. R., Randolph, S. S., Cheson, B. D. (2008) Phase II trial of oral vorinostat (suberoylanilide hydroxamic acid) in relapsed diffuse large-B-cell lymphoma. *Ann. Oncol.* **19**, 964–969.
40. Kalac, M., Scotto, L., Marchi, E., Amengual, J., Seshan, V. E., Bhagat, G., Ulahannan, N., Leshchenko, V. V., Temkin, A. M., Parekh, S., Tycko, B., O'Connor, O. A. (2011) HDAC inhibitors and decitabine are highly synergistic and associated with unique gene-expression and epigenetic profiles in models of DLBCL. *Blood* **118**, 5506–5516.
41. Chen, R., Frankel, P., Popplewell, L., Siddiqui, T., Ruel, N., Rotter, A., Thomas, S. H., Mott, M., Nathwani, N., Htut, M., Nademanee, A., Forman, S. J., Kirschbaum, M. (2015) A phase II study of vorinostat and rituximab for treatment of indolent non-Hodgkin lymphoma (newly diagnosed and relapsed/refractory). *Haematologica* **3**, 357–362.
42. Fernández-Rodríguez, C., Salar, A., Navarro, A., Gimeno, E., Pairet, S., Camacho, L., Ferraro, M., Serrano, S., Besses, C., Bellosillo, B., Sanchez-Gonzalez, B. (2015) Antitumor activity of the combination of bendamustine with vorinostat in diffuse large B-cell lymphoma cells. *Leuk. Lymphoma* **18**, 1–25.
43. Yang, J., Kuang, X. R., Lv, P. T., Yan, X. X. (2015) Thymoquinone inhibits proliferation and invasion of human nonsmall-cell lung cancer cells via ERK pathway. *Tumour Biol.* **36**, 259–269.
44. Chen, C. Y., Chung, I. H., Tsai, M. M., Tseng, Y. H., Chi, H. C., Tsai, C. Y., Lin, Y. H., Wang, Y. C., Chen, C. P., Wu, T. I., Yeh, C. T., Tai, D. I., Lin, K. H. (2014) Thyroid hormone enhanced human hepatoma cell motility involves brain-specific serine protease 4 activation via ERK signaling. *Mol. Cancer* **13**, 162.
45. D'Cruz, O. J., Uckun, F. M. (2013) Protein kinase inhibitors against malignant lymphoma. *Expert Opin. Pharmacother.* **14**, 707–721.
46. Infante, E., Ridley, A. J. (2013) Roles of Rho GTPases in leucocyte and leukemia cell transendothelial migration. *Philos. Trans. R. Soc. Lond. B Biol. Sci.* **368**, 20130013.
47. Guo, F., Velu, C. S., Grimes, H. L., Zheng, Y. (2009) Rho GTPase Cdc42 is essential for B-lymphocyte development and activation. *Blood* **114**, 2909–2916.
48. Zhang, H., Schaff, U. Y., Green, C. E., Chen, H., Sarantos, M. R., Hu, Y., Wara, D., Simon, S. I., Lowell, C. A. (2006) Impaired integrin-dependent function in Wiskott-Aldrich syndrome protein-deficient murine and human neutrophils. *Immunity* **25**, 285–295.
49. Gérard, A., Mertens, A. E., van der Kammen, R. A., Collard, J. G. (2007) The Par polarity complex regulates Rap1- and chemokine-induced T cell polarization. *J. Cell Biol.* **176**, 863–875.
50. Lakshmaiah, K. C., Jacob, L. A., Aparna, S., Lokanatha, D., Saldanha, S. C. (2014) Epigenetic therapy of cancer with histone deacetylase inhibitors. *J. Cancer Res. Ther.* **10**, 469–478.
51. Valenzuela-Fernández, A., Cabrero, J. R., Serrador, J. M., Sánchez-Madrid, F. (2008) HDAC6: a key regulator of cytoskeleton, cell migration and cell-cell interactions. *Trends Cell Biol.* **18**, 291–297.
52. Ding, N., Ping, L., Feng, L., Zheng, X., Song, Y., Zhu, J. (2014) Histone deacetylase 6 activity is critical for the metastasis of Burkitt's lymphoma cells. *Cancer Cell Int.* **14**, 139.
53. Namdar, M., Perez, G., Ngo, L., Marks, P. A. (2010) Selective inhibition of histone deacetylase 6 (HDAC6) induces DNA damage and sensitizes transformed cells to anticancer agents. *Proc. Natl. Acad. Sci. USA* **107**, 20003–20008.

54. Wang, S., Yan-Neale, Y., Fischer, D., Zeremski, M., Cai, R., Zhu, J., Asselbergs, F., Hampton, G., Cohen, D. (2003) Histone deacetylase 1 represses the small GTPase RhoB expression in human nonsmall lung carcinoma cell line. *Oncogene* **22**, 6204–6213.
55. Wang, Y., Zhou, Y., Graves, D. T. (2014) FOXO transcription factors: their clinical significance and regulation. *BioMed Res. Int.* **2014**, 925350.
56. Hagenbuchner, J., Kuznetsov, A., Hermann, M., Hausott, B., Obexer, P., Ausserlechner, M. J. (2012) FOXO3-induced reactive oxygen species are regulated by BCL2L1 (Bim) and SESN3. *J. Cell Sci.* **125**, 1191–1203.
57. Rohde, M., Richter, J., Schlesner, M., Betts, M. J., Claviez, A., Bonn, B. R., Zimmermann, M., Damm-Welk, C., Russell, R. B., Borkhardt, A., Eils, R., Hoell, J. I., Szczepanowski, M., Oschlies, I., Klapper, W., Burkhardt, B., Siebert, R.; German ICGC MMML-Seq-Project; NHL-BFM Study Group. (2014) Recurrent RHOA mutations in pediatric Burkitt lymphoma treated according to the NHL-BFM protocols. *Genes Chromosomes Cancer* **53**, 911–916.
58. Hu, Y., Ou, Y., Wu, K., Chen, Y., Sun, W. (2012) miR-143 inhibits the metastasis of pancreatic cancer and an associated signaling pathway. *Tumour Biol.* **33**, 1863–1870.
59. Huang, M., Prendergast, G. C. (2006) RhoB in cancer suppression. *Histol. Histopathol.* **21**, 213–218.
60. Connolly, E. C., Van Doorslaer, K., Rogler, L. E., Rogler, C. E. (2010) Overexpression of miR-21 promotes an in vitro metastatic phenotype by targeting the tumor suppressor RHOB. *Mol. Cancer Res.* **8**, 691–700.
61. Liu, M., Tang, Q., Qiu, M., Lang, N., Li, M., Zheng, Y., Bi, F. (2011) miR-21 targets the tumor suppressor RhoB and regulates proliferation, invasion and apoptosis in colorectal cancer cells. *FEBS Lett.* **585**, 2998–3005.
62. Sato, N., Fukui, T., Taniguchi, T., Yokoyama, T., Kondo, M., Nagasaka, T., Goto, Y., Gao, W., Ueda, Y., Yokoi, K., Minna, J. D., Osada, H., Kondo, Y., Sekido, Y. (2007) RhoB is frequently downregulated in non-small-cell lung cancer and resides in the 2p24 homozygous deletion region of a lung cancer cell line. *Int. J. Cancer* **120**, 543–551.
63. Liu, A., Prendergast, G. C. (2000) Geranylgeranylated RhoB is sufficient to mediate tissue-specific suppression of Akt kinase activity by farnesyltransferase inhibitors. *FEBS Lett.* **481**, 205–208.
64. Bousquet, E., Mazières, J., Privat, M., Rizzati, V., Casanova, A., Ledoux, A., Mery, E., Couderc, B., Favre, G., Pradines, A. (2009) Loss of RhoB expression promotes migration and invasion of human bronchial cells via activation of AKT1. *Cancer Res.* **69**, 6092–6099.
65. Kazerounian, S., Gerald, D., Huang, M., Chin, Y. R., Udayakumar, D., Zheng, N., O'Donnell, R. K., Perruzzi, C., Mangiante, L., Pourat, J., Phung, T. L., Bravo-Nuevo, A., Shechter, S., McNamara, S., Duhadaway, J. B., Kocher, O. N., Brown, L. F., Toker, A., Prendergast, G. C., Benjamin, L. E. (2013) RhoB differentially controls Akt function in tumor cells and stromal endothelial cells during breast tumorigenesis. *Cancer Res.* **73**, 50–61.

KEY WORDS:

non-Hodgkin lymphoma · Rho GTPase · histone deacetylase inhibitor · phosphoinositide 3-kinase inhibitor